Macromolecules **2003,** *36,* 7721−7729

Self-Organizing Polycondensation of (*E*)-4-Acetoxycinnamic Acid for Preparation of Poly(*p*-oxycinnamoyl) Microspheres

Kunio Kimura,*,† Hiromasa Inoue,† Shin-ichiro Kohama,† Yuhiko Yamashita,† and Yoshimitsu Sakaguchi‡

Faculty of Environmental Science and Technology, Okayama University, 3-1-1 Tsushima-naka, Okayama 700-8530, Japan, and Toyobo Research Center Co. Ltd., 1-1 Katata 2-Chome, Ohtsu, Shiga 520-0292, Japan

Received April 1, 2003

ABSTRACT: Preparation of poly(*p*-oxycinnamoyl) (POC) microspheres was examined by the reaction-induced phase separation of oligomers during the polycondensation of (*E*)-4-acetoxycinnamic acid in various solvents. Polymerization in liquid paraffin yielded the microspheres having a smooth surface at 270−330 °C, of which the average diameter was 4.6 μm. In contrast to this, the morphology of the products was drastically changed in Therm S 800 (TS8) and Therm S 900 (TS9) by polymerization temperature. When the polymerization was carried out at 310 °C in TS8 and 300 °C in TS9, the microspheres were obtained, of which the average diameter was 3.9 and 3.3 μm, respectively. The platelike crystals were formed under these temperatures, of which thickness was approximately 0.1 μm. The formation of the microspheres was highly related to the miscibility between the oligomers and the solvents. The average diameter of the microspheres increased with the decrease of the miscibility, and this tendency could be accounted for by the interfacial tension between two immiscible liquid phases. The microspheres were formed through the formation of the microdroplets by the liquid−liquid phase separation of the oligomers and the subsequent solidification of the microdroplets due to the further polymerization in them.

Introduction

Wholly aromatic polymers possess many excellent properties such as thermal stability, mechanical properties, and chemical resistance. Therefore, they have been widely used as high-performance materials. However, the processing of these materials is generally more difficult than for conventional flexible chain polymers due to strong enthalpic interactions and the minimal increase in conformational entropy associated with their dissolution or melting. The relationship between properties and processability is a tradeoff, and numerous trials have been conducted to overcome this antagonistic problem from the aspect of not only chemical modification of polymer structures[1] but also processing techniques.[2]

We have been studying the morphology control of rigid polymers during polymerization to overcome the above antagonistic problem and succeeded in preparing the whiskers of poly(*p*-oxybenzoyl) and other aromatic polyesters.[3−11] The poly(*p*-oxybenzoyl) whiskers are prepared by the polymerization of *p*-acetoxybenzoic acid in liquid paraffin (LPF) with the elimination of acetic acids. These whiskers are formed through the reaction-induced crystallization of oligomers during solution polymerization. The formation mechanism of these whiskers contains the following three steps which are the precipitation of oligomers to form the lamellae, the spiral growth of the lamellae as needlelike shape caused by the screw dislocation, and the further polymerization in the needlelike crystals.[4] These studies provide the new methodology for the morphology control of the rigid aromatic polymers, and many other kinds of whiskers have been prepared so far.[12−15]

Scheme 1. Synthesis of POC from ACA

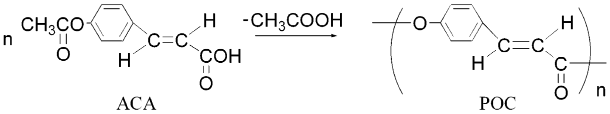

Poly(*p*-oxycinnamoyl) (POC) is also a rigid-rod aromatic polyester comprised of *p*-vinylphenyl group and ester linkage as illustrated in Scheme 1. Although POC is also expected to be a hopeful candidate for high-performance materials, it exhibits neither solubility nor meltability. Therefore, copolyesters containing *p*-oxycinnamoyl moiety had been prepared as thermotropic polymers so far,[16,17] but POC has not been used as materials. To overcome this poor processability, the reaction-induced phase separation of oligomers is an applicable method to control the morphology of POC.

This paper describes our new findings on the morphology control of POC by the reaction-induced phase separation of oligomers during the polycondensation of (*E*)-4-acetoxycinnamic acid (ACA).

Experimental Section

Materials. Predominantly (*E*)-4-hydroxycinnamic acid (HCA) and (*E*)-cinnamoyl chloride were purchased from Aldrich Co. Ltd. Benzophenone (BPN) was purchased from Ishizu Seiyaku Ltd. and used as obtained. LPF was purchased from Nacalai Tesque Co. Ltd. and purified by vacuum distillation (220−240 °C/0.3 mmHg). Therm-S 900 (TS9) and Therm-S 800 (TS8), which were aromatic heat exchange media, were purchased from Nippon Steel Chemical Co. Ltd. TS8 and TS9 were the mixture of triethylbiphenyl and hydrogenated terphenyl, respectively. They were purified by vacuum distillation (TS8: 140−160 °C/0.5 mmHg; TS9: 150−170 °C/0.7 mmHg). (*E*)-4-Acetoxycinnamic acid (ACA) was synthesized according to the previously reported procedure.[16,17]

Polymer Synthesis. A typical polymerization procedure was described as follows. Into a cylindrical vessel equipped

---

† Okayama University.

‡ Toyobo Research Center Co. Ltd.

* To whom correspondence should be addressed. Tel & Fax: +81-86-251-8902; e-mail: polykim@cc.okayama-u.ac.jp.

10.1021/ma030197q CCC: $25.00

with a mechanical stirrer and a gas inlet tube were placed 0.30 g of ACA (1.46 mmol) and 20 mL of LPF (1.5% w/v). The reaction mixture was heated under a slow stream of nitrogen up to 320 °C with stirring. The stirring was stopped when ACA was completely dissolved. The temperature was maintained at 320 °C for 6 h. The precipitated products were collected by vacuum filtration at 320 °C and washed with *n*-hexane and acetone. Product characteristics were as follows. FT-IR (KBr) (cm^{-1}): 2920 (aromatic CH), 1725 (ester C=O), 1633 (vinyl C=C). Anal. Calcd for $C_9H_6O_2$: C, 73.97; H, 4.14; O, 21.89. Found: C, 74.94; H, 4.21; O, 20.85.

Synthesis of Phenyl (*E*)-4-[(*E*)-Cinnamoyloxy]cinnamate (PCC). Into a 50 mL flask equipped with a dropping funnel, a thermometer and a gas inlet tube were placed 1.00 g of HCA (6.10 mmol), 0.74 g of triethylamine (7.32 mmol), and 20 mL of dried tetrahydrofuran. A solution of 1.22 g of (*E*)-cinnamoyl chloride (7.32 mmol) and 10 mL of dried tetrahydrofuran was added dropwise through the dropping funnel under the slow stream of nitrogen at 5 °C. The reaction temperature was kept at 5 °C for 2 h and then at 25 °C for 12 h. The reaction mixture was filtrated to remove the triethylamine−HCl salts and acidified by diluted HCl solution. The white precipitates were collected and washed with water. Recrystallization from ethyl acetate/*n*-hexane gave 1.10 g (76%) of white crystals of (*E*)-4-[(*E*)-cinnamoyloxy]cinnamic acid. The purity was checked by HPLC. Product characteristics were as follows. T_m: 206 °C. FT-IR (KBr) (cm^{-1}): 3300−2500 (OH), 1735 (ester C=O), 1693 (carboxylic acid C=O), 1627 (vinyl C=C). Anal. Calcd for $C_{18}H_{14}O_4$: C, 73.46; H, 4.79; O, 21.75. Found: C, 73.53; H, 4.75; O, 21.72. ^{1}H NMR ($CDCl_3$/CF_3COOH; δ, ppm): 7.42−7.48 (H-1, H-2, m, 3H), 7.59−7.64 (H-3, H-7, m, 4H), 7.96 (H-4, d, 1H, $J = 16.0$ Hz), 6.67 (H-5, d, 1H, $J = 16.0$ Hz), 7.24 (H-6, d, 2H, $J = 7.2$ Hz), 7.85 (H-8, d, 1H, $J = 16.0$ Hz), 6.45 (H-9, d, 1H, $J = 16.0$ Hz).

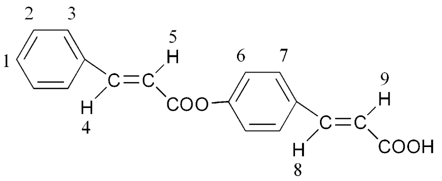

^{13}C NMR ($CDCl_3$/CF_3COOH; δ, ppm): 131.86 (C-1), 129.42 (C-2), 128.61 (C-3), 133.98 (C-4), 149.44 (C-5), 116.22 (C-6), 167.83 (C-7), 152.99 (C-8), 122.77 (C-9), 130.36 (C-10), 132.08 (C-11), 148.40 (C-12), 116.55 (C-13), 173.79 (C-14).

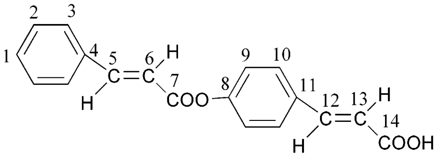

Into a 50 mL flask equipped with HCl gas trap were placed 0.50 g of (*E*)-4-[(*E*)-cinnamoyloxy]cinnamic acid and 15 mL of thionyl chrolide. Three drops of *N*,*N*-dimethylformamide were added into the reaction mixture, and the mixture was stirred at 25 °C for 12 h. The excess of thionyl chloride was stripped off, and recrystallization from dried *n*-hexane gave 0.53 g (67%) of (*E*)-4-[(*E*)-cinnamoyloxy]cinnamoyl chloride (67%). FT-IR (KBr) (cm^{-1}): 1741 (acid chloride C=O), 1721 (ester C=O), 1629 (vinyl C=C).

Into a 100 mL flask equipped with a dropping funnel, a thermometer and a gas inlet tube were placed 0.09 g of phenol (0.96 mmol) and 20 mL of dried tetrahydrofuran. A solution of 0.15 g of (*E*)-4-[(*E*)-cinnamoyloxy]cinnamoyl chloride (0.48 mmol) was added at 5 °C under a slow stream of nitrogen. A solution of 0.06 g of triethylamine (0.96 mmol) and 5 mL of dried tetrahydrofuran was added dropwise through the dropping funnel at 5 °C. The reaction temperature was kept at 5 °C for 2 h and then 25 °C for 12 h. The reaction mixture was filtrated to separate the triethylamine−HCl salts and acidified by diluted HCl solution. The white precipitates were collected and washed with water. Recrystallization from ethyl acetate/*n*-hexane gave 0.145 g (82%) of white crystals of PCC. The purity was checked by HPLC. Product characteristics were as follows. T_m: 158 °C. FT-IR (KBr) (cm^{-1}): 1735 (ester C=O), 1631 (vinyl C=C). Anal. Calcd for $C_{24}H_{18}O_4$: C, 77.82; H, 4.90; O, 17.28. Found: C, 77.31; H, 4.81; O, 17.88. ^{1}H NMR ($CDCl_3$/CF_3COOH; δ, ppm): 7.39−7.49 (H-1, H-2, H-11, m, 5H), 7.63 (H-3, d, 2H, $J = 7.8$ Hz), 7.98 (H-4, d, 1H, $J = 16.0$ Hz), 6.66 (H-5, d, 1H, $J = 16.0$ Hz), 7.26 (H-6, d, 2H, $J = 8.0$ Hz), 7.68 (H-7, d, 2H, $J = 8.0$ Hz), 7.95 (H-8, d, 1H, $J = 16.0$ Hz), 6.69 (H-9, d, 1H, $J = 16.0$ Hz), 7.15 (H-10, d, 2H, $J = 8.0$ Hz), 7.29 (H-12, t, 1H, $J = 8.0$ Hz).

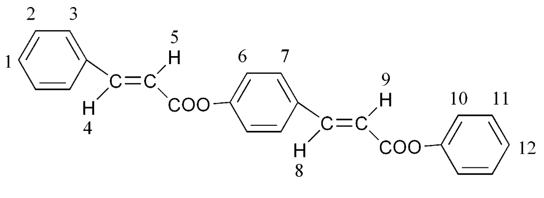

^{13}C NMR ($CDCl_3$/CF_3COOH; δ, ppm): 131.92 (C-1), 129.52 (C-2), 129.06 (C-3), 133.96 (C-4), 149.59 (C-5), 116.15 (C-6), 168.10 (C-7), 152.84 (C-8), 122.81 (C-9), 130.35 (C-10), 132.37 (C-11), 147.73 (C-12), 117.05 (C-13), 168.85 (C-14), 150.58 (C-15), 121.82 (C-16), 130.11 (C-17), 126.98 (C-18).

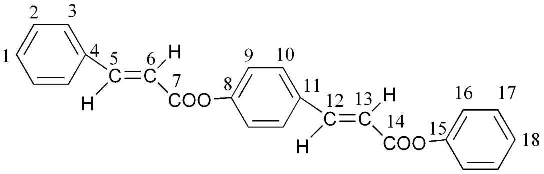

Measurements. Morphology of the polymer crystals was observed by scanning electron microscopy (S-2150, Hitachi Co. Ltd.) at 20 kV. FT-IR spectra were measured on a FT-IR spectrometer (FT/IR-410, JASCO Co. Ltd.). The chemical structures of ACA and the oligomer model compounds were characterized by ^{1}H and ^{13}C NMR (Bruker AVANCE500) operating at 500 MHz (^{1}H) and 125 MHz (^{13}C). The NMR spectra were measured in $CDCl_3$/CF_3COOH. Signal assignments were carried out with the help of C−H COSY spectra and the spectral data of cinnamic acid described in the Integrated Spectral Data Base System for Organic Compounds (SDBS) presented by the National Institute of Advanced Industrial Science and Technology (AIST), Japan. The chemical structure of POC was characterized by solid-state ^{13}C NMR (Bruker AVANCE500) operating at 75 MHz. The purity of oligomer model compounds was checked by HPLC (Waters 600E-490E system) with a Nova Pack HR C18 column. The eluent was a mixture of water containing 2 wt % acetic acid and acetonitrile, and the mixing volume ratio of these two solvents was changed linearly from 90/10 to 0/100 for 40 min. The WAXS pattern was measured by a diffractometer (Gaiger flex, Rigaku Co. Ltd.) with nickel-filtered Cu Kα radiation (35 kV, 20 mA). Thermal stability was measured on a Perkin-Elmer TGA 7 at a heating rate of 20 °C min^{-1} in a nitrogen atmosphere. T_g and T_m were measured on a Perkin-Elmer DSC 7 at a scanning rate of 10 °C min^{-1} in a nitrogen atmosphere. The densities of the microspheres were measured by the flotation method using tetrachloromethane and *p*-xylene at 25 °C. The diameter of the microspheres was determined by the average of over 100 observation values.

Determination of Number-Average Degree of Polymerization of Polymers. 10 mg of sample and 1 mL of 7.0 wt % potassium hydroxide methanol solution were placed in a test tube and kept at 25 °C until the sample was completely hydrolyzed to HCA. The solution was neutralized with dilute hydrochloric acid and then analyzed by using gas chromatography (GC-14B Shimadzu Co. Ltd.) with a Thermon-3000 (60−80 mesh) packed column. Number-average degree of polym-

Table 1. Polymerization Results of ACA in Various Solvents[a]

solvent	T_s (°C)[b]	polymerization temp (°C)	T_b (°C)[c]	t_t (min)[d]	morphology
LPF	195	270−330		25 (290 °C), 10 (320 °C)	spherical
TS9	165	270−290	290−300	40 (290 °C)	platelike
		300−330		25 (320 °C)	spherical
TS8	155	280−300	300−310	50 (290 °C)	platelike
		310−330		40 (320 °C)	spherical
BPN	136	270−300		60 (290 °C)	platelike

[a] Polymerizations were carried out at a concentration of 1.5% w/v for 5 h. [b] T_s is the temperature at which ACA is completely dissolved. [c] T_b is the boundary temperature at which the morphology of the product changes from platelike crystals to microspheres. [d] t_t is the time when the solution becomes turbid. Temperature in parentheses shows the polymerization temperature.

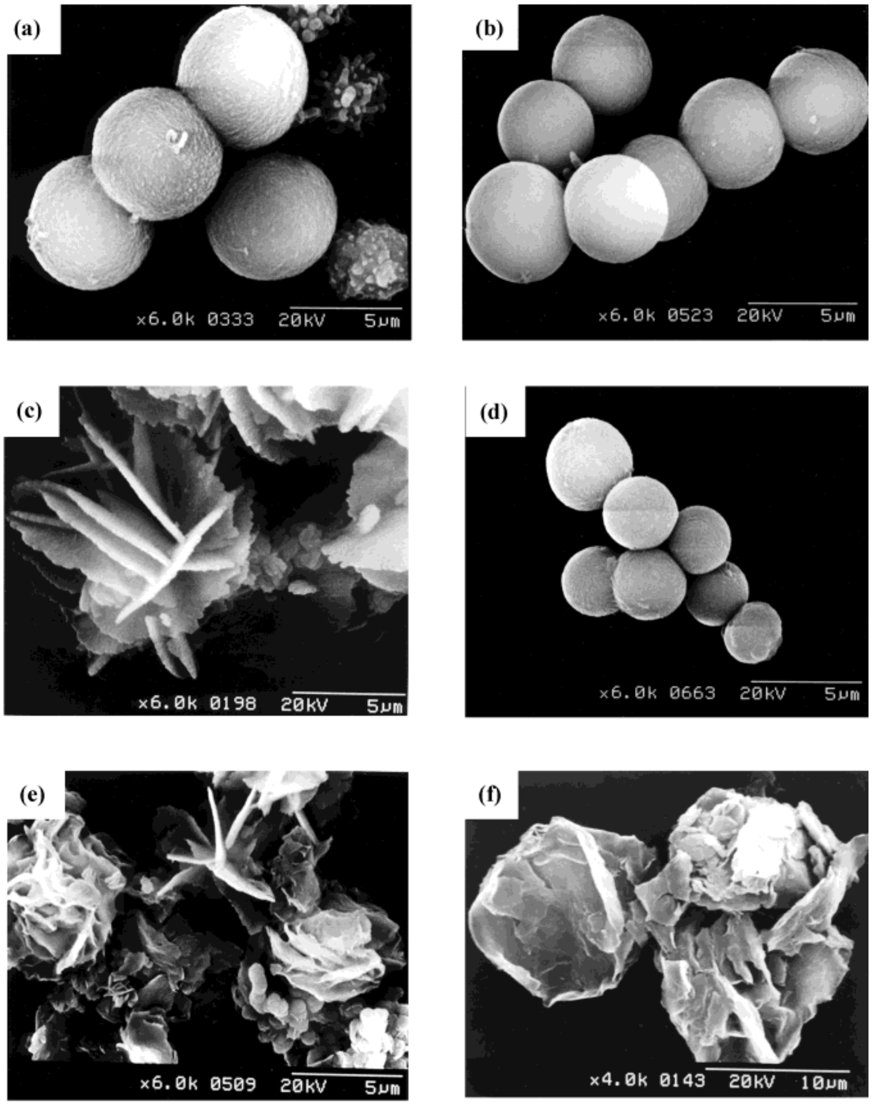

Figure 1. Morphology of POC prepared for 5 h (a) in LPF at 320 °C, (b) in TS9 at 320 °C, (c) in TS9 at 280 °C, (d) in TS8 at 320 °C, (e) in TS8 at 280 °C, and (f) in BPN at 290 °C.

erization (DP_n) of the polymer was calculated by the molar ratio of HCA and acetic acid.

Preparation of Phase Diagrams of Oligomer Model Compounds. PCC and the solvent were put into glass tubes at different concentrations. They were placed into oil bath and heated until PCC was completely dissolved. Then temperature was lowered gradually at a rate of 5 °C h^{-1}, and the cloud point temperatures were determined. The phases and conjugate line between the liquid and solid phases were confirmed by microscope equipped with a heating stage (MP-500D, Yanaco Co. Ltd.) under crossed polarization.

Measurement of Reaction Rate. Reaction kinetics was measured by the modified procedure reported previously.[18] Into the 40 mL cylindrical vessel equipped with gas inlet and outlet tubes were placed 0.30 g of ACA (1.46 mmol) and 20 mL of the solvents. The mixtures were placed into an oil bath and heated to 320 °C under a slow stream of nitrogen with stirring. By-produced acetic acid was trapped in the water at different time. The polymerization was followed with measuring the concentration of evolved acetic acid. In the case of LPF, the concentration of evolved acetic acid was monitored until 7 min when the precipitation of the oligomers began. In the cases of TS9, it was monitored until 20 min. The amount of acetic acid produced at a given time was determined by titration with 0.1 mol L^{-1} sodium hydroxide solution. The reactions obeyed the second-order kinetics, and the rate constants (k_2) were estimated from the plots of evolved acetic acid as a function polymerization time.

Results and Discussion

Morphology of POC. Polymerizations of ACA were carried out under several conditions, and Table 1 summarizes the results of the polymerizations. In all cases, the clear solution became turbid at the early stage of polymerization due to the precipitation of oligomers, and then the products were gradually formed. Figure 1 shows the morphology of the products. Polymerization in LPF does not yield the crystals having clear habit. The microspheres having smooth surface are formed at the polymerization temperature of 270−330 °C, of which the diameter is 3−5 μm. The obtained microspheres can be separated by ultrasonication in the solution. In the contrast to LPF, the morphology of POC is drastically changed in TS9 by the polymerization temperature. When the polymerization is carried out under 290 °C, only platelike crystals are formed, of which the thickness is approximately 0.1 μm. On the other hand, the microspheres having smooth surface are formed over 300 °C. It is very interesting that the platelike crystals are never formed over 300 °C. The morphology appeared in TS8 is very similar to that in TS9; that is, the platelike crystals are formed under 300 °C, and the microspheres are formed over 310 °C. In BPN, only the platelike crystals are obtained in the temperature range 270−300 °C. The polymerization could not be carried out over 300 °C in BPN because of its boiling temperature. The boundary polymerization temperature (T_b) at which the morphology is drastically changed from plate to sphere exists at 290−300 °C in TS9 and 300−310 °C in TS8. T_b's in LPF and BPN are anticipated to exist under 270 °C and over 300 °C, respectively. These morphological features reveal that the platelike crystals, and the microspheres are formed through the different mode of the phase separation of oligomers during polymerization; that is, the former is formed by the crystallization of oligomers, and the latter is formed by the liquid−liquid phase separation of oligomers. The existence of T_b in TS9 and TS8 supports the above discussion.

POC is insoluble into any organic solvents, and hence the chemical structure is analyzed by FT-IR and solid-state ^{13}C NMR measurements. FT-IR spectra were measured to confirm the chemical structure. Figure 2 illustrates the spectra of ACA and the microspheres prepared in TS9 at 320 °C. C═O stretching peaks of carboxylic acid and acetoxy group at 1693 and 1749 cm^{-1} in the spectrum of ACA disappeared significantly in the spectrum of the microspheres. The O−H stretching peak of carboxylic acid at 3300−2500 cm^{-1} in the spectrum of ACA also disappeared in the spectrum of the microspheres. The C═O stretching peak in ester linkage appeared newly at 1725 cm^{-1} in the spectra of the microspheres. C═C stretching peak is found at 1633 cm^{-1} in both spectra, and this indicates that the C═C group of the *p*-vinylphenyl moiety remains unchanged during high-temperature polymerization. Figure 3 is a CP/MAS/TOSS ^{13}C NMR of POC microspheres prepared in TS9 at 320 °C. The peaks of vinyl carbon are detected at 113 and 147 ppm, respectively. This spectrum shows the formation of POC. These results confirm that the microspheres are comprised of POC. Figure 4 shows the WAXS profile of the microspheres. The diffraction peaks are sharp. The diffuse halo attributed to amorphous parts is slightly observed. It is obvious that the microspheres possess high crystallinity. Some diffraction peaks can be accounted for, as illustrated in Figure 4, according to the previously reported POC unit cell constants which are as follows: orthorhombic, $a = 0.82$ nm, $b = 0.48$ nm, c is unknown.[19] Thermal properties of the microspheres were evaluated. Thermal decomposition temperatures of 5 wt % loss and 10 wt % loss in nitrogen are 415 and 428 °C, respectively. The microspheres exhibit neither glass transition temperature due to high crystallinity nor melting temperature under the thermal decomposition temperature on the DSC profile. These microspheres show excellent thermal stability.

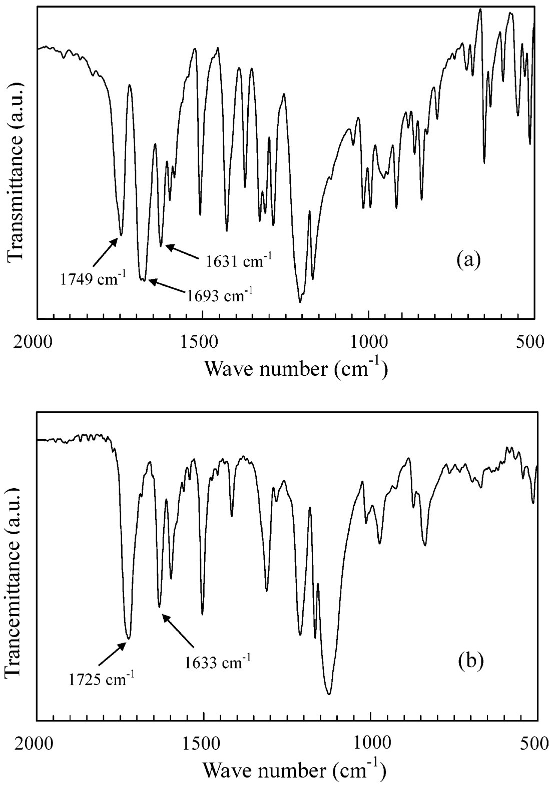

Figure 2. FT-IR spectra of (a) ACA and (b) POC microspheres prepared in TS9 at 320 °C for 5 h.

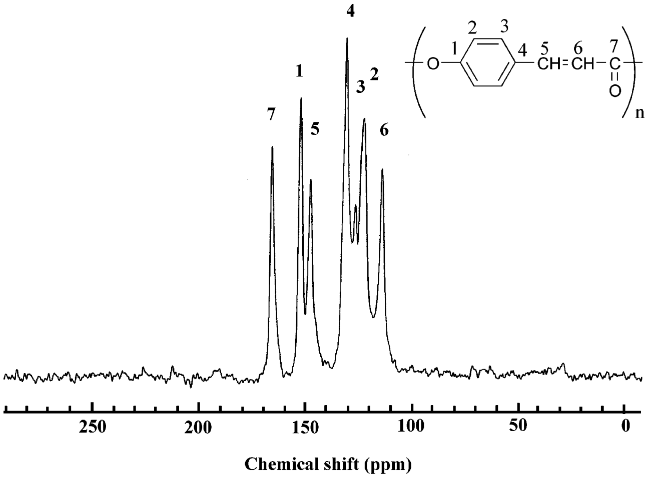

Figure 3. CP/MAS/TOSS ^{13}C NMR spectrum of POC microspheres prepared in TS9 at 320 °C.

The formation of the microspheres is significantly controlled by not only the solvent but also the polymerization temperature, and the miscibility between the oligomer and the solvent seems to be a determining factor. The temperature at which ACA is completely dissolved (T_s) can be adopted as a criterion to evaluate

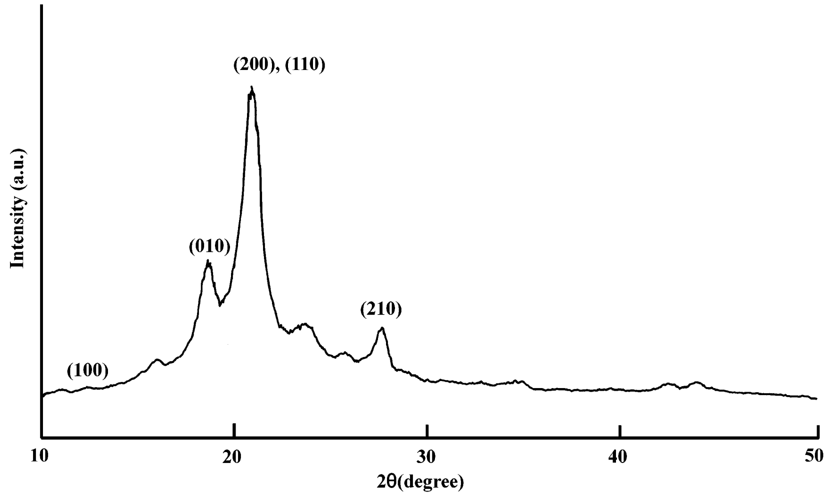

Figure 4. WAXS profile of microspheres prepared in TS9 at 320 °C for 5 h.

the miscibility. The time when the polymerization becomes turbid (t_t) can be also used to estimate the miscibility. T_s increases in the order of BPN, TS8, TS9, and LPF, and t_t decreases in the same order of T_s as shown in Table 1. These results suggest that the miscibility between the oligomer and the solvent increases in order of LPF, TS9, TS8, and BPN. Here, the solubility parameters (δ) of ACA, POC, and the solvents are compared to evaluate the miscibility more qualitatively. The δ's of LPF, TS9, and TS8 used here are appeared in the previous study,[20] and those of ACA, POC, and BPN are estimated by Fedors' group contribution method.[21] The δ's of LPF, TS9, TS8, and BPN are 8.28, 9.54, 9.70, and 11.24 (cal cm^{-3})$^{1/2}$, respectively. Those of ACA and POC are 10.76 and 11.20 (cal cm^{-3})$^{1/2}$, respectively. These results reveal that the miscibility increases in order of LPF, TS9, TS8, and BPN, which is in good agreement with the order estimated by T's and t_t. The temperature range in which the microspheres are formed becomes wider, and T_b shifts toward lower temperature with the decrease of miscibility.

To better-understand the influence of solvent on the formation of the microspheres, the phase separation behavior is considered. Reaction-induced phase separation of oligomers in poor solvent is describable on the analogous concentration−temperature phase diagram (*CT* phase diagram) to that of partially miscible polymer−solvent system.[22,23] The phase separation curve in the repulsive system in which there is no attractive interaction between the oligomer and the solvent can be written as the combination of the freezing point curve of the oligomers and the upper critical solution temperature type consolute curve. Figure 5 depicts the schematic illustration of the phase diagram. The oligomers are formed by the condensation reaction of ACA, and the DP$_n$ of the oligomers increases in the solution. When the DP$_n$ of the oligomers exceeds a critical value, they are in the supersaturation state and then phase-separated. If the supersaturated oligomers are across the freezing point curve, they are precipitated by the crystallization to form the crystals. On the other hand, if across the consolute curve, the oligomers are precipitated through liquid−liquid phase separation and the microdroplets of the dense phase are generated in the dilute phase because the volume fraction of the dense phase is quite low. Finally, polymer microspheres are formed due to the solidification of the microdroplets caused by the further polymerization in them. The reaction-induced liquid−liquid phase separation in this case is the binordal decomposition, and it does not occur through spinodal decomposition. To compare the phase separation behavior of the oligomers, the location of the phase separation curve in LPF and TS9 is considered by the division of the phase separation curve into the freezing point curve and the consolute curve. The oligomers are insoluble into common organic solvents under the temperature at which the polymerization starts, and the phase-separated oligomers cannot be isolated. Hence, the consolute curve and the freezing point curve of the phase-separated oligomer cannot be accurately determined. The relative location of these curves is discussed with a clue of the miscibility. With respect to the freezing point curves, they are influenced by both the DP$_n$ of the phase-separated oligomers and their depression. To compare, the DP$_n$ of the phase-separated oligomers was estimated as the average DP$_n$ of the dissolved oligomers when the phase separation started. The polymerization reactions were followed by the titration of evolved acetic acid with aqueous NaOH.

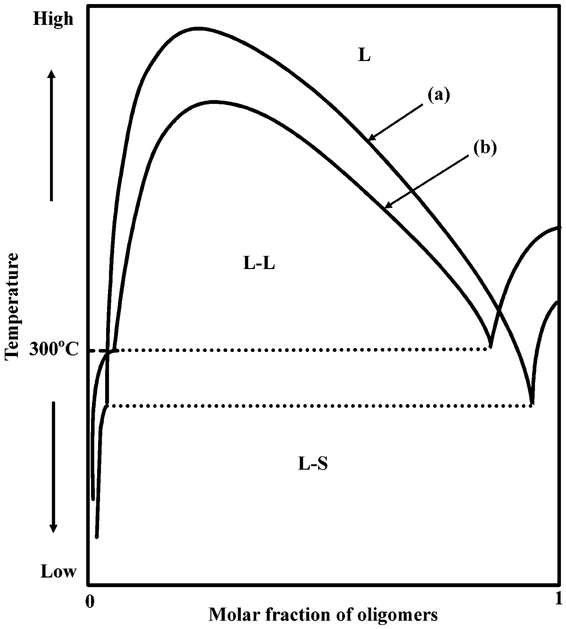

Figure 5. Schematic illustration of CT phase diagrams for the system of (a) oligomer LPF and (b) oligomer TS9. L = miscible liquid phase; L−L = immiscible two liquid phases; L−S = liquid and solid phase.

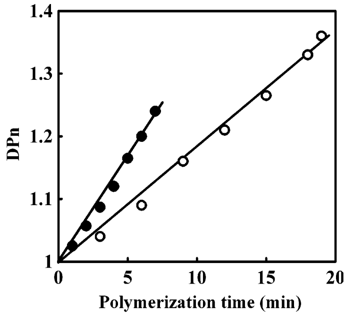

Figure 6. Plots of DP_n as a function of polymerization time in the polymerization of ACA in LPF (●) and TS9 (○) at 320 °C. Initial concentration of ACA is 0.073 mol L^{-1}.

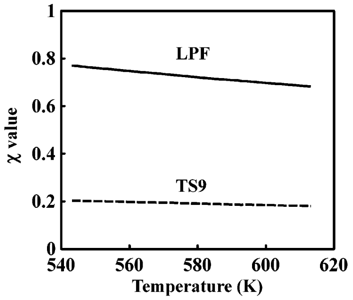

Figure 7. Temperature dependency of χ parameters between POC and solvents.

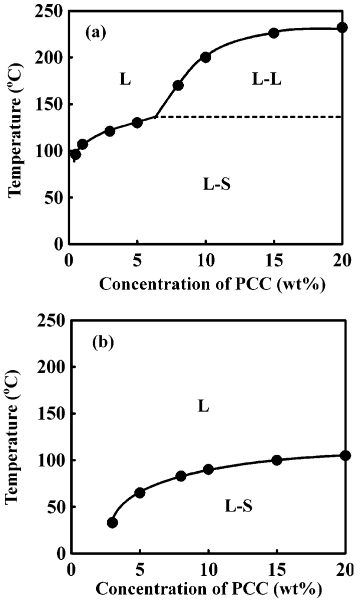

Figure 8. Phase diagrams of (a) PCC−LPF and (b) PCC−TS9. L, L−L, and L−S appear in Figure 5.

Table 2. Average Diameter and Coefficient of Variation of POC Microspheres

polymerization[a]			
solvent	temp (°C)	av diam (μm)	coeff of variation (%)
LPF	320	4.61	5
TS9	320	3.94	9
TS8	320	3.32	10

[a] Polymerizations were carried out at a concentration of 1.5% w/v for 5 h.

Figure 6 plots the DP_n of the oligomers as a function of the polymerization time. Reactions obeyed the second-order kinetics, and k_2's at 320 °C in LPF and TS9 were estimated from the slopes as 0.56 and 0.26 L mol^{-1} min^{-1}, respectively. On the basis of these k_2's and t_t's, the average DP_n's of the oligomers dissolved in the solution when the precipitation starts can be estimated as 1.24 in LPF and 1.36 in TS9. The average DP_n of the oligomers is much lower in LPF than that in TS9. This fact indicates that the lower DP_n oligomers are phase-separated in LPF rather than in TS9. It is well-known that the freezing point of oligomers is a function of DP_n, and it increases with the DP_n due to mainly the decrease of an entropy change for the coagulation.[24,25] Depression of the freezing point is also highly related to the miscibility, and it might be larger in TS9 than in LPF. The depression of the freezing point at very low concentration cannot be accurately estimated in both solvents. Although there exists still unclear part about the depression of the freezing point, it can be speculated that the freezing point curve of the phase-separated oligomers in LPF is relatively located toward lower temperature on *CT* phase diagram. With respect to the relative location of the consolute curves, χ parameters are estimated with the δ's discussed before by the following equation:[26]

$$\chi_{12} = (Vr/RT)(\delta_1 - \delta_2)^2$$

where Vr is the segment molar volume of POC, δ_1 is the solubility parameter of POC, and δ_2 is the solubility parameter of solvent. Here, Vr is calculated by Fedors' group contribution method.[21] Figure 7 shows the calculation curve of χ parameters as a function of temperature. Although the estimated χ parameters are not accurate values because Fedors' group contribution method includes some assumptions for the calculation, they can be used to compare the miscibility. The χ value between POC and LPF is larger than that between POC and TS9 over the polymerization temperature range from 270 to 330 °C. It can be thought that the lower miscibility makes the consolute curve shift toward higher temperature on the *CT* phase diagram. As a result, the shifts of both the consolute curve and the freezing point curve extend the two immiscible liquids phase on the *CT* phase diagram in LPF as shown in Figure 5, and therefore the temperature range for the formation of the microspheres becomes wider in LPF than TS9. The boundary line between two immiscible liquids phase and liquid−solid phase must exist at ca. 300 °C in TS9. To confirm the above discussion, PCC was synthesized as a oligomer model compound, and the *CT* phase diagrams were prepared by the cloud point measurements. Figure 8 shows the *CT* phase diagram of PCC and LPF and that of PCC and TS9. The phase separation curve appears as the combination of the freezing point curve and the consolute curve, and the two immiscible liquids phase is clearly observed in LPF. On the other hand, only the freezing point curve appears up to the concentration of 20 wt % in TS9. The comparison of these diagrams reveals that the consolute curve in LPF shifts largely toward higher temperature, and the two immiscible liquids phase is more widely expanded. This result strongly substantiates the above discussion.

Table 2 summarizes the average diameter of the microspheres prepared in several solvents at 320 °C for 5 h. The diameters of the microspheres are highly dependent on the solvent. Those prepared in LFP, TS9, and TS8 are 4.61, 3.94, and 3.32 μm with the coefficient of variation of 5−10%. This result exhibits that the diameter decreases with the miscibility. The formation mechanism of the microspheres is the nucleation and growth mechanism as discussed before. The detail is discussed in the following section. It seems likely that the diameter of the microspheres is governed by the two processes, of which one is the nucleation process and another is the growth process. With respect to the nucleation process, it is well-known that the critical radius of nucleus (r^*) and nucleation rate (J) depend on the degree of supersaturation as follows:[27,28]

$$\Delta\mu = kT\ \ln(1 + \sigma)\sigma = (C - C_e)/C_e$$

$$r^* = 2v\gamma/\Delta\mu$$

$$J = \nu_+ q\ \exp(-\Delta G^*/kT) = \nu_+ q\ \exp(-16\pi\gamma^3 v^2/3\Delta\mu^2 kT)$$

where μ is the chemical potential, C the concentration of solute, C_e the equilibrium concentration, r^* the critical radius of nucleus, v the volume of the molecule, γ the density of surface energy, J the nucleation rate, ν_+ the rate of crystallization of one molecule into the critical nucleus, and q the density of the free molecule. When the degree of supersaturation (σ) increases, $\Delta\mu$ which is a driving force for nucleation becomes larger. This large $\Delta\mu$ leads to small r^* and large J, indicating that much more nuclei having a smaller radius are formed. The σ is highly related to the miscibility between the oligomer and the solvent, and the lower miscibility results in the larger σ. The lower miscibility of LPF makes the σ larger. Additionally, the higher formation rate of the oligomers in LPF, as shown before, also causes the larger σ. Thereby, the largest number of the nuclei is generated in LPF leading to the smaller diameter, and the diameter is likely to increase with the miscibility. However, the results are not in agreement with this discussion, and the tendency is totally opposite. This disagreement indicates that the diameter is not governed by the nucleation process and done by the growth process. This tendency can be qualitatively understood on the basis of the difference in the interfacial tension. The interfacial tension (γ_i) is determined by the miscibility of two phases, and it can be described in the strong phase-separated system by the Flory–Huggins mean-field approximation as follows:[29–31]

$$\gamma_i \propto (kT/v_0)a\chi^{1/2}$$

where v_0 is the lattice volume, a the segment length, and T the temperature. The above relation means that γ_i becomes larger in the less miscible system, and therefore the diameter of the microspheres increases with the decrease of the miscibility.

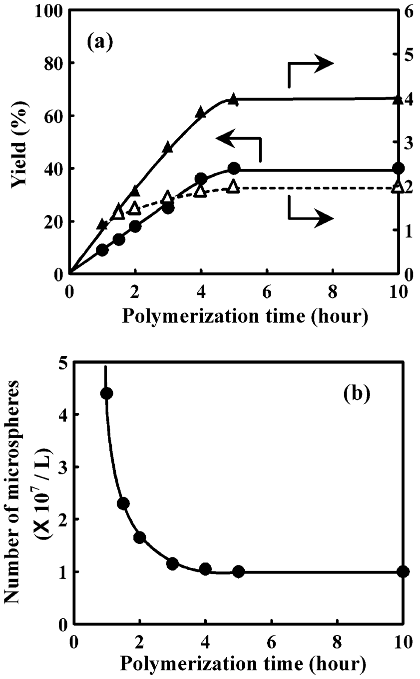

Figure 9. Polymerization time dependency of (a) yield (●), diameter (▲), and (b) number of microspheres prepared in TS9 at 320 °C. The diameter calculated from the yield assuming that the number of microspheres is constant (△) is also shown in (a).

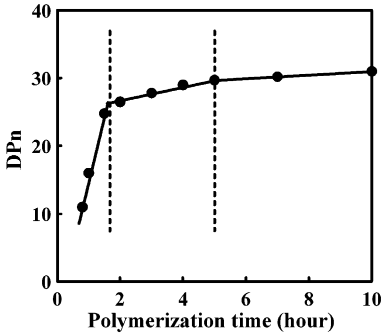

Figure 10. Plot of DP$_n$ of microspheres prepared in TS9 at 320 °C as a function of polymerization time.

Growth Mechanism of POC Microspheres. The yield and the average diameter of the microspheres were followed in the course of the polymerization in TS9 at 320 °C. The number of the microspheres was calculated with the yield, the diameter, and the density of the microspheres, which was 1.38 g cm^{-3}. Figure 9 plots the results as a function of the polymerization time. The yield increases with the polymerization time, and this shows that the microspheres are grown by the consecutive supply of the oligomers from the solution. The yield is saturated at 40% after 5 h, and it is not quantitative. The oligomers were scarcely left in the solution at 5 h, and therefore the low yield is due to the sublimation of ACA. The diameter of the microspheres also increases with the yield. But the increment of the diameter is much larger than that calculated on the basis of the yields assuming that the number of the microsphere is constant. This fact indicates that there exists another mechanism of the diameter increase besides the supply of the oligomers. The number of the microspheres decreases very rapidly at the early stage of polymerization, and then it becomes constant after 4 h. This rapid decrease suggests strongly that the microdroplets formed through liquid–liquid phase separation of the oligomers coalesce each other at the early stage of polymerization. Figure 10 shows the change in the DP$_n$ of the microspheres. The DP$_n$ increases rapidly until 2 h. The concentration of the end groups becomes higher in the microdroplets, and therefore the further polycondensation proceeds rapidly at the early stage of polymerization. From 2 to 5 h, the slope of the DP$_n$ increment decreases because the oligomers in the microdroplets lose their chain mobility due to the increase of the DP$_n$ as observed in the melt polymerization of aromatic polyesters.[18,32] During this period, the crystallization is induced in the microdroplets, so-called solidification, by the increase of the freezing point of the oligomers due

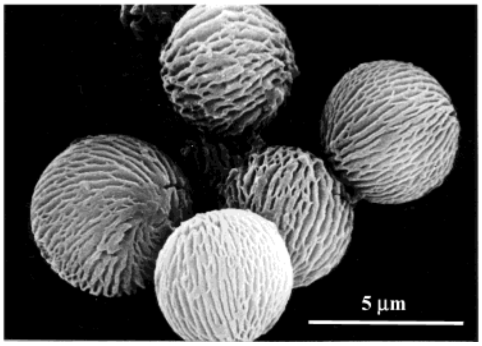

Figure 11. Inner structure of microspheres etched by aqueous KOH solution. The microspheres were prepared in TS9 at 320 °C for 10 h.

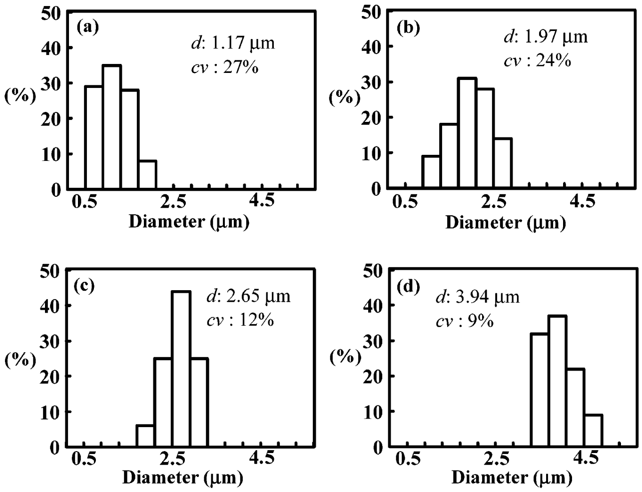

Figure 12. Diameter distribution diagrams of POC microspheres prepared in TS9 at 320 °C for (a) 1, (b) 2, (c) 3, and (d) 5 h. *d* and *cv* stand for an average diameter and a coefficient of variation, respectively.

to the increase of DP_n. This solidification changes the microdroplets to the microspheres, and it makes the surface stable. Then the coalescence of the microdroplets stops, which is in good agreement with Figure 9b. After 5 h when the yield is leveled off, the DP_n increases slightly due to the solid-state polymerization in the microspheres. To know the inner structure of the microspheres, those prepared in TS9 at 320 °C for 10 h were etched by 5.0 mol L^{-1} aqueous KOH solution. Figure 11 shows the etched microspheres. The diameter of the etched microspheres is close to that of the as polymerized microspheres, and hence the surface layer of the microspheres is removed by etching. The sheaflike morphology is clearly observed, and the thickness of the coagulated platelike crystals is approximately 0.2 μm. This inner structure is developed during the solidification. The diameter distribution diagrams of the microspheres prepared in TS9 at 320 °C are shown in Figure 12. The diameter increases with the polymerization time showing a unimodal distribution. Once the microdroplets are formed by the nucleation, the oligomers phase-separated thereafter are consumed to grow the microdroplets. The coefficient of variation for the diameter distribution varies from 26.5% to the smaller value of 9.1% in the course of the polymerization. This result indicates the possibility of an alternate growth route of the microspheres, that is, Ostwald ripening. The small droplets disappear by dissolution due to the disadvantage of the surface energy. However, the molecular weight of the oligomers increases rapidly in the microdroplets at the early stage of the polymerization as described, and this increase results in the lack of the solubility of oligomers. Thereby, the possibility of the Ostwald ripening process cannot be completely excluded, but this may not be a major growth process of the microspheres.

Conclusions

The POC microspheres are obtained by the self-organizing polycondensation of ACA in LPF, TS8, and TS9. These microspheres possess the outstanding thermal stability. The diameter of the microspheres, which is in the range 3.3−4.6 μm, is dependent on the solvents, and it increases with the decrease of the miscibility between the solvent and the oligomers. They are formed through the formation of the microdroplets by the liquid−liquid phase separation of oligomers and the subsequent polymerization in the microdroplets leading to the solidification of the microdroplets due to the increase of molecular weight. They are grown by not only the consecutive supply of the oligomers from the solution but also the coalescence of the microdroplets. This result provides the new methodology for preparing the microspheres of the intractable aromatic polymers.

References and Notes

(1) For example: Cassidy, P. E. *Thermally Stable Polymers, Syntheses and Properties*; Marcel Dekker: New York, 1980. Blumstain, A. *Liquid Crystalline Order in Polymers*; Acadenic Press: London, 1978.
(2) For example: Seymour, R. B.; Kirshenbaum, G. S. *High Performance Polymers; Their Origin and Development*; Elsevier: New York, 1986.
(3) Yamashita, Y.; Kimura, K. *Polymeric Materials Encyclopedia*; CRC Press: Boca Raton, FL, 1996; p 8707.
(4) Yamashita, Y.; Kato, Y.; Endo, S.; Kimura, K. *Makromol. Chem. Rapid Commun.* **1988**, *9*, 687.
(5) Kato, Y.; Endo, S.; Kimura, K.; Yamashita, Y.; Tsugita, H.; Monobe, K. *Koubunnshi Ronbunshu* **1987**, *44*, 35.
(6) Yamashita, Y.; Kato, Y.; Endo, S.; Kimura, K.; Tsugita, H.; Monobe, K. *Koubunnshi Ronbunshu* **1987**, *44*, 41.
(7) Kato, Y.; Yamashita, Y.; Kimura, K.; Endo, S.; Ohta, T. *Koubunnshi Ronbunshu* **1990**, *47*, 583.
(8) Kimura, K.; Endo, S.; Kato, Y.; Yamashita, Y. *Polymer* **1993**, *35*, 123.
(9) Kimura, K.; Yamashita, Y. *Polymer* **1994**, *35*, 3311.
(10) Kimura, K.; Endo, S.; Kato, Y.; Yamashita, Y. *Polymer* **1993**, *34***,** 1054.
(11) Kimura, K.; Kato, Y.; Inaba, T.; Yamashita, Y. *Macromorecules* **1995**, *28*, 255.
(12) Kricheldorf, H. R.; Schwarz, G.; Ruhser, F. *Macromorecules* **1991**, *24*, 3485.
(13) Kricheldorf, H. R.; Struve, O.; Schwarz, G. *Polymer* **1996**, *37*, 4311.
(14) Kricheldorf, H. R.; Schwarz, G.; Adebahr, T.; Wilson, D. J. *Macromolecules* **1993**, *26*, 6622.
(15) Schwarz, G.; Kricheldorf, H. R. *Macromolecules* **1995**, *28*, 3911.
(16) Krigbaum, W. R.; Ishikawa, T.; Watanabe, J.; Toriumi, H.; Kubota, H.; Preston, J. *J. Polym. Sci., Polym. Phys. Ed.* **1983**, *21*, 1851.
(17) Kricheldorf, H. R.; Stukenbrock, T. *Makromol. Chem.* **1997**, *198*, 3753.
(18) Williams, P. A.; Han, H.; Padias, A. B.; Hall, Jr., H. K. *Macromolecules* **1996**, *29*, 1874.
(19) Tugita, H.; Yokoyama, F.; Yamashita, Y. *Sen-i Gakkaishi* **1994**, *50*, 256.
(20) Tate, S.; Watanabe, Y.; Chiba, A. *Polymer* **1993**, *34*, 4974.
(21) Fedors, R. F. *Polym. Eng. Sci.* **1974**, *14*, 147.
(22) Richards, R. B. *Trans. Faraday Soc.* **1946**, *42*, 10.
(23) Flory, P. J.; Mandelkern, L.; Hall, H. K. *J. Am. Chem. Soc.* **1951**, *73*, 2532.
(24) Mita, I.; Yokota, R.; Kambe, H. *Rep. Prog. Polym. Phys. Jpn.* **1971**, *16*, 319.

(25) Kojima, Y.; Ichinose, K.; Nakamura, T.; Hosaka, N. *Kobunsi Ronbunshu* **1978**, *35*, 629.
(26) Flory, P. J. *Principles of Polymer Chemistry*; Cornell University Press: Ithaca, NY, 1953.
(27) Burton, W. K.; Cabrera, N.; Frank, F. C. *Philos. Trans. R. Soc. London, Ser. A* **1950**, *243*, 299.
(28) Frank, F. C. *Adv. Phys.* **1952**, *1*, 91.
(29) Helfand, E.; Tagami, Y. *J. Chem. Phys.* **1972**, *56*, 3592.
(30) Helfand, E.; Sapse, A. M. *J. Chem. Phys.* **1975**, *62*, 999.
(31) Nose, T. *Polym. J.* **1975**, *8*, 96.
(32) Lodha, A.; Ghadage, R. S.; Ponrathnam, S. *Polymer* **1997**, *38*, 6167.

MA030197Q